Prebiotic Chemistry

International Edition: DOI: 10.1002/anie.201902997
German Edition: DOI: 10.1002/ange.201902997

# Charge Transport through Self-Assembled Monolayers of Monoterpenoids

*Brian J. Cafferty, Li Yuan, Mostafa Baghbanzadeh, Dmitrij Rappoport, M. Hassan Beyzavi, and George M. Whitesides**

**Abstract:** *The nature of the processes at the origin of life that selected specific classes of molecules for broad incorporation into cells is controversial. Among those classes selected were polyisoprenoids and their derivatives. This paper tests the hypothesis that polyisoprenoids were early contributors to membranes in part because they (or their derivatives) could facilitate charge transport by quantum tunneling. It measures charge transport across self-assembled monolayers (SAMs) of carboxyl-terminated monoterpenoids ($O_2C(C_9HX)$) and alkanoates ($O_2C(C_7HX)$) with different degrees of unsaturation, supported on silver ($Ag^{TS}$) bottom electrodes, with $Ga_2O_3$/EGaIn top electrodes. Measurements of current density of SAMs of linear length-matched hydrocarbons—both saturated and unsaturated—show that completely unsaturated molecules transport charge faster than those that are completely saturated by approximately a factor of ten. This increase in relative rates of charge transport correlates with the number of carbon–carbon double bonds, but not with the extent of conjugation. These results suggest that polyisoprenoids—even fully unsaturated—are not sufficiently good tunneling conductors for their conductivity to have favored them as building blocks in the prebiotic world.*

Polyisoprenoids—also known as terpenoids—are a class of molecules found in all domains of life. At the cellular level, they serve both metabolic and structural roles.[1] Were polyisoprenoids selected for multiple functions (for example, the ability to conduct charge) at the beginning of life, or purely for their availability and activity as surfactants?[2] Charge transport (CT) is important to a number of biological redox networks,[3] and its appearance in peri-biotic systems—whatever their nature—was probably important for the emergence of life.[4] This work examines the relation between structure and rate of CT by tunneling across polyisoprenoids (both fully saturated and unsaturated), and addresses the question of whether rates of CT through polyisoprenoids that are fast (relative to other lipids) have contributed to their selection as molecular components of early living systems.

Little is known about CT through polyisoprenoids and, more specifically, about tunneling through molecules that have C=C bonds that are not conjugated. We examined the relative rates of charge transport by tunneling through SAMs of alkanoates on template-stripped silver, and varied the number of C=C bonds from zero (completely saturated) to three (completely unsaturated). Comparison of current density and UPS (ultraviolet photoelectron spectroscopy) shows that the number of C=C bonds correlates with the rate of charge transport by a statistically significant, but small, amount (a factor of 16 increase in rates of tunneling with complete unsaturation). Two limiting possibilities might contribute to this increase: i) The average height of the tunneling barrier might decrease with unsaturation. ii) The geometry or length of the molecule (or the thickness of the SAM) might correspondingly change in a way that decreases the width of the tunneling barrier. We conclude that the former is the more probable explanation, and suggest that the ability of polyisoprenoids to support transport by charge tunneling is unlikely to have been a reason why they were selected by evolution as components of archaea and other early organisms, and, we presume, of peri-biotic vesicles.[2a,c]

Most studies of trends in tunneling current density, $J$ ($A\,cm^{-2}$), with molecular structure across SAM-based junctions[5] have been characterized in terms of the simplified (and largely empirical, as it is commonly used) Simmons equation [Eq. (1)].[6] As qualitatively interpreted, $\beta$ is the tunneling decay coefficient and is related to the mean height of the barrier, $d$ is the width of the tunneling barrier, and $J_0$ is the value of the current density extrapolated to $d = 0$. Two models commonly used to rationalize the observation that some molecules have significantly larger rates of tunneling than length-matched alkanes include i) coherent tunneling, which involves reducing the energy off-set between molecular frontier orbitals (the highest occupied molecular orbitals (HOMO) or the lowest unoccupied molecular orbitals (LUMO) and the work function of the electrodes), and ii) "superexchange tunneling," which involves molecular orbitals formed by non-bonding interactions among high-energy occupied orbitals.[7]

[*] Dr. B. J. Cafferty, Dr. L. Yuan, Dr. M. Baghbanzadeh, Dr. D. Rappoport, Prof. M. H. Beyzavi, Prof. G. M. Whitesides
Department of Chemistry and Chemical Biology, Harvard University
12 Oxford Street, Cambridge, MA 02138 (USA)
E-mail: gwhitesides@gmwgroup.harvard.edu
Prof. G. M. Whitesides
Kalvi Institute for Bionano Science and Technology
Harvard University
29 Oxford Street, Cambridge, MA 02138 (USA),
and
Wyss Institute for Biologically Inspired Engineering
Harvard University
60 Oxford Street, Cambridge, MA 02138 (USA)
Prof. M. H. Beyzavi
Current address: Department of Chemistry and Biochemistry, University of Arkansas, Fayetteville, AR 72701 (USA)
Supporting information and the ORCID identification number(s) for the author(s) of this article can be found under https://doi.org/10.1002/anie.201902997.

  

$$J(V) = J_0(V)e^{-\beta d} \quad (1)$$

The first mechanism—coherent tunneling—has been studied by several groups, including that of Frisbie, who examined transport through SAMs of oligophenylene or polythiophene attached to gold by a metal–thiolate bond via conductive atomic force microscopy (cAFM),[8] and of Chiechi, who examined junctions of SAMs of molecules with fully conjugated oligophenylene groups.[9] These studies found that the rate of charge transport through fully conjugated molecules is up to factor of $10^3$ larger than molecules of similar length with only partial or no conjugated orbital systems. McCreery, Bergren, and co-workers, however, examined rates of charge transfer across a series of different aromatic molecules and established that the rates changed only modestly (by a factor of ten) with large differences in their HOMO energies ($>2$ eV).[10] On introducing a single methylene group between the anchoring thiol and a oligophenol group ($SCH_2(Ph)_n$ versus $S(Ph)_n$), we observed a significant decrease in the rate of charge transport (from a value of $\beta$ of $0.28 \pm 0.03$ Å$^{-1}$ for the completely conjugated molecules to a value of $\beta$ of $0.66 \pm 0.06$ Å$^{-1}$ for the partially conjugated molecules).[5i] This finding suggests that the rate of tunneling is sensitive to disruption in delocalization of molecular orbitals between the molecules and the $Au_nS$ interface.

The second mechanism, proposed by McConnell, Ratner, and Nitzan—"superexchange tunneling"—describes hole tunneling in unconjugated, or partially conjugated orbital system that involves interactions among high-energy occupied orbitals.[7] We have rationalized that CT through SAMs of oligomers of glycine, $(Gln)_n$, sarcosine $(Src)_n$, and ethylene glycol, $(EG)_n$, as proceeding through hole tunneling by superexchange.[11] This process involves interactions among the high-energy occupied orbitals of either the amide groups in $(Gln)_n$ or $(Src)_n$, or the ether oxygen atoms in $(EG)_n$. The variation in tunneling rates for SAMs of $(Gln)_n$ with length ($\beta = 0.44 \pm 0.01$ Å$^{-1}$), and of $(EG)_n$ ($\beta = 0.24 \pm 0.01$ Å$^{-1}$), are comparable to those of SAMs of length-matched oligophenyls, which have partially conjugated π-orbital systems. Unlike conjugated molecular systems, however, $(Gly)_n$- and $(EG)_n$-based systems can have lone pairs of electrons that are separated by intervening saturated groups.

This study describes CT across junctions of the form: $Ag^{TS}$/SAM//$Ga_2O_3$/EGaIn, where $Ag^{TS}$ is template-stripped silver,[12] the SAM is formulated either from a monoterpenoid, an n-alkanoate, or an n-alkenoate (Table 1), EGaIn is eutectic gallium–indium alloy, and $Ga_2O_3$ is a conductive thin film of gallium oxide. This type of junction has been described elsewhere in detail.[13] We examine CT across 3,7-dimethyl-2,6-octadienoic acid (geranic acid, **3**) and related molecules that are either saturated or contain C=C bonds in different positions along the monoterpene backbone (see Table 1 for structures). We used carboxylates instead of thiolates as anchoring groups for three reasons: i) they limit delocalization of orbitals across the interface,[5i] ii) alkanes with terminal carboxylates have been proposed to be plausible components of protocell membranes,[14] and iii) they can form densely packed SAMs,[9] which—to some extent—mimic the lipid membranes of vesicles.[15] To understand the influence of a single C=C bond on CT, we compare current density across these monoterpenoids to octanoic acid—a length-matched hydrocarbon—and to analogs of octanoic acid that contain a single C=C bond at different positions along the hydrocarbon backbone (see Table 1 for structures). We use angle-dependent X-ray photoelectron spectroscopy (ADXPS) to characterize the structure of the SAMs,[16] and ultraviolet photoelectron spectroscopy (UPS) to characterize the work function of the Ag/SAM interface and HOMO energy of the SAMs.[17] Density functional theory (DFT) provides some understanding of the theoretical mechanism of tunneling through these molecules.[18]

***Table 1:*** Summary of XPS, UPS, and current density measurements for molecules **1**–**9**.

| | Molecule | Work function (eV)[a] ±0.1 | HOMO (eV)[b] ±0.1 | log\|J\| +0.5 V[c,d,e] |
|---|---|---|---|---|
| **1** | 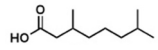 | 4.3 | −6.4 | 0.1 ± 0.4 |
| **2** | 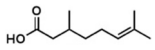 | 4.3 | −6.4 | 0.5 ± 0.2 |
| **3** | 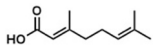 | 4.3 | −6.3 | 1.0 ± 0.2 |
| **4** | 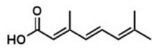 | 4.3 | −6.1 | 1.3 ± 0.1 |
| **5** | 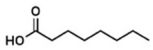 | 4.3 | −6.4 | 0.4 ± 0.4 |
| **6** | 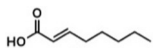 | 4.3 | −6.4 | 0.5 ± 0.3 |
| **7** | 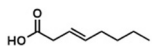 | 4.3 | −6.4 | 0.6 ± 0.4 |
| **8** | 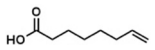 | 4.3 | −6.4 | 0.6 ± 0.2 |
| **9** | 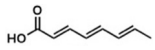 | 4.3 | −6.1 | 1.2 ± 0.1 |

[a] Values of work function were determined by UPS. [b] The energy level of the HOMO (the orbital assignments are in Table S1) with respect to the energy level of vacuum, estimated by UPS. [c] log|J| is the log of the current density (J) at +0.5 V. Units of J are A cm$^{-2}$. [d] log|J| at −0.5 V and rectification ratios are given in Table S2. [e] Junctions shorted at ±1.0 V. Compounds **1**–**4** were tested at ±1.0 V, but after one or two unstable scans the junctions shorted. The scans that were acquired did not rectify.

*Electronic and structural characterization of the SAMs.* We determined the thickness, $d$ (in nm), of the nine monolayers using ADXPS. The values of $d$ (Figure S1) show that the nine monolayers have similar thickness (values of thickness are between 0.7 and 0.8 nm, ±0.1 nm), which are comparable to the previously reported thickness ($d = 0.9$ nm) of octanoic acid on $Ag^{TS}$.[19] This observation suggests the SAMs (of molecules **1**–**9**) were formed with a similar quality, despite differences in saturation, and perhaps in conformation along the carbon backbone. Physisorbed molecules, such as solvent molecules, were not observed in the monolayers by XPS (Figures S2 and S3).

Using UPS, we characterized the electronic structure of SAMs formed from both the monoterpenoid series (molecules **1**–**4**) and the octanoic acid series (molecules **5**–**9**), in terms of work function and energy of the HOMO (Figure 1). There is no statistically significant difference in the work function of any compound.

  

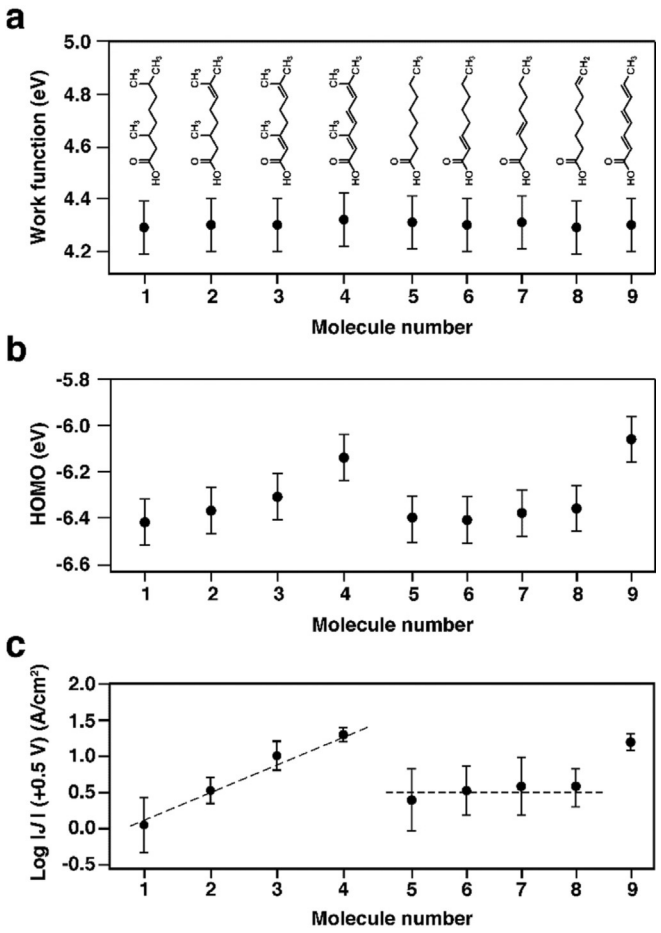


***Figure 1.*** a) Plot of the work functions of Ag supporting SAMs (**1**–**9**) determined by UPS. b) Plot of the HOMO energies for molecules **1**–**9** determined by UPS. Error bars in (a) and (b) are 0.1 eV, which was the energy resolution of the UPS spectra. c) Plot of mean values of $\log|J|$ at + 0.5 V for molecules **1**–**9**. Error bars represent the standard deviation of mean values. Numbers on the X-axis correspond to molecules shown in Table 1. The dashed lines are guides for the eye. See Figure S8 for number of data (N) collected. Rectification of current was not observed between +0.5 V and −0.5 V (see Table S2 for rectification ratios).

The values of the energy of the HOMOs for SAMs of both the monoterpenoid and octanoic acid series show different trends. For the monoterpenoid series, the value of the orbital energy increases with an increase in the number of C=C bonds (from zero in molecule **1** to three in molecule **4**). This trend may reflect the delocalization of the HOMO from localized on the carboxylate group (molecule **1**), to being fully extended through the backbone (molecule **4**). As the number of C=C bonds increases, the peaks in the UPS spectra broaden and overlap, over the range of binding energy from 0 to 5 eV (Figures S4 and S5). These spectral features suggest greater delocalization of the HOMO as the number of C=C bonds increases. Molecule **4** is completely unsaturated, and its HOMO is delocalized over the entire backbone (see section on DFT calculations). As a result, its HOMO is 0.3 eV higher than compound **1**. Using energy values of the HOMO obtained by UPS, we constructed an energy level diagram for compounds **1** to **4** (Figure S6) which suggests a decrease in the height of the energy barrier with increasing unsaturation.

For the octanoic acid series, the energy level of the HOMO for SAMs composed of molecules **5** to **8** is nearly constant at −6.4 eV, but increases to −6.0 eV for the SAM of the fully unsaturated **9**. For the monounsaturated molecules of the octanoic acid series (molecules **6**–**8**), only the positions of one C=C bond with respect to the terminal group (COOH) are different, and the energy of the HOMO is unchanged. The energy level diagram in Figure S7 shows no distinguishable difference in the energy levels of the HOMO and LUMO for molecules **6**–**8**. These results suggest that the position of the double bond in the hydrocarbon backbone does not change the energy level of the HOMO and LUMO.

*Current Density Measurements of SAMs of the Monoterpenoid Series.* We measured $J(V)$ curves for junctions of the form $Ag^{TS}/SAM//Ga_2O_3/EGaIn$ over the range of $\pm 0.5$ V (Figure S8) and compared the values of $\log|J|$ at +0.5 V (Table 1 and Figure 1c). The differences in $\log|J|$ for the four monoterpenoids (**1**–**4**) increased with the number of C=C bonds ($\log|J|$ for 3,7-dimethyl-2,6-octadienoic acid (**3**) and 3,7-dimethyloctanoic acid (**1**) differed by approximately ×8). The highest $\log|J|$ value of this series was recorded for the completely unsaturated 3,7-dimethyl-2,4,6-octatrienoic acid (**4**, $\log|J| = 1.3 \pm 0.1$), which showed a factor of $16 \pm 3$ greater rate of tunneling than **1** ($\log|J| = 0.1 \pm 0.4$). The observation that increasing the number of C=C bonds increases the value of $\log|J|$ is consistent with UPS data, and with the proposed decrease in the average height of the energy barrier with increasing unsaturation.

*DFT Calculations of the Monoterpenoid Series.* DFT (Turbomole with B3LYP hybrid exchange-correlation functional) helped correlate the experimental measurements of tunneling conductance with changes in the molecular structure of the SAM for molecules **1**–**4**.[20] The HOMO in the unsaturated monoterpenoids are the C=C bond orbitals or COOH group orbitals, which include the in-plane orbitals from the lone pair on the oxygen and the out-of-plane orbitals from the π bond of the carbonyl (Table S1). The HOMO of the unsaturated monoterpenoids are located on the π bonds of the internal C=C bonds (Figure 2). The interactions between these C=C bonds range from weak in 3,7-dimethyl-6-octenoic acid (**2**) and 1,5-unsaturated 3,7-dimethyl-2,6-octadienoic acid (**3**, 0.16 eV), to strong in the fully conjugated 3,7-dimethyl-2,4,6-octatrienoic acid (**4**, 1.17 eV).

For molecules **1**–**3** in which the HOMO is not delocalized over the entire molecule, it is possible that the next highest occupied energy level (HOMO−1) could contribute to the height of the total barrier. Figure 2 shows that the energy of HOMO−1 increases with increasing unsaturation for molecules **1**–**3**. This increase correlates with an increase in the rate of charge transport for these compounds. We previously found a similar correlation between the energy of the HOMO−1 and the rate of charge transport across SAMs of oligoglycine and oligoethylene glycol.[11] These calculations suggest that charge transport through **1**–**3** might be influenced by occupied molecular orbitals that are lower in energy than the HOMO.

  

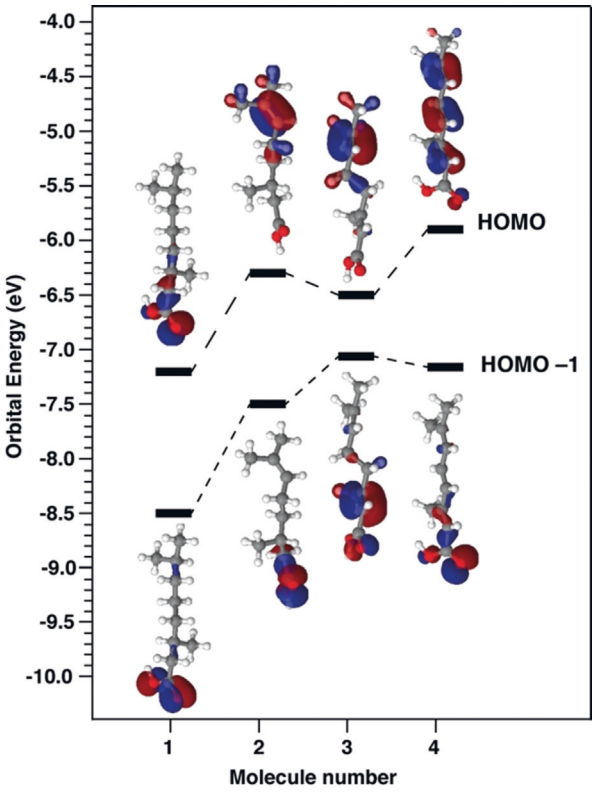


***Figure 2.*** Orbital energies (HOMO and HOMO−1) and shapes of orbitals of the monoterpenoid series (molecule **1** to **4**) from DFT calculations in the gas phase. The solid bars are the orbital energies and the dashed lines are guides for the eyes. See Table S1 for list of additional adjacent occupied orbitals.

We also determined the end-to-end length of these monoterpenoids using structures optimized by DFT. Specifically, we measured the terminal carbon of the carboxylate to the terminal proton of the head group (i.e., the proton in contact with the EGaIn electrode). These measurements show a 5% change in length between molecule **1** (9.92 Å) and molecule **3** (9.42 Å) which correlates with an increase in the degree of unsaturation (Figure S9). Using the Simmons equation [Eq. (1)] and $\beta$ determined experimentally for linear alkanoates ($\beta = 0.78$ Å$^{-1}$),[19] we estimate that this difference in length would increase the current density by $\times 1.5$ for molecule **3**. The difference in $\log|J|$ for molecule **1** and **3** determined by current density measurements ($\Delta\log|J| = 0.9 \pm 0.6$) shows an increase in current density of approximately $\times 8$. The increased rate of tunneling with increasing unsaturation for molecules **2** and **3** is due, in part, to a decrease in the width of the tunneling barrier, but the effect is small.

*Current Density Measurements of SAMs of the Octanoic Acid Series.* We also studied a second series of molecules: octanoic acid (**5**) and related unsaturated molecules (**6**–**9**). These molecules have the same length (in terms of carbon atoms) as the monoterpenoid series, but do not include methyl side groups, and may have different conformations in the SAM. Figure 1c shows that compound **9** showed the only statistically significant difference in these $\log|J|$ values (log $|J| = 1.2 \pm 0.2$). We conclude from the set of molecules **1**–**9** that increasing the degree of unsaturation, but not the position of the C=C bond (**6**–**8**), influences the rate of tunneling through length-matched hydrocarbons.

This study demonstrates that current density of SAMs of length-matched hydrocarbons increases with the degree of unsaturation (with an increase of $\times 16$ going from **1** to **4**). Current density and HOMO energies measurements show trends that support a linear increase in the rate of tunneling with increasing unsaturation (molecules **1**–**4**). The position of the C=C bond did not influence the rate of tunneling, as molecules with a single C=C bond at different positions along the carbon backbone had comparable rates (molecules **6**–**8**). From measurements of current density, transition voltage analysis shows that the tunneling mechanism does not change as a function of the applied voltages across the junctions (Figure S10). The data do not identify a mechanism for tunneling, but two factors might contribute. i) The length of the molecule slightly decreases with unsaturation, with a 5% decrease in length for molecule **3** compared to molecule **1** corresponding to a $\times 1.5$ increase in current density as estimated by the Simmons equation [Eq. (1)]. ii) The mean height of the tunneling barrier decreases with unsaturation, due to an increase in the energy of the highest occupied molecular orbitals, with a decrease of the tunneling barrier of $\approx 0.3$ eV for the fully unsaturated molecule **4** compared to the fully saturated molecule **1**. Figure 3 shows correlations between $\log|J|$ and the number of double bonds, and $\log|J|$ and the energy of the HOMO determined by UPS. These

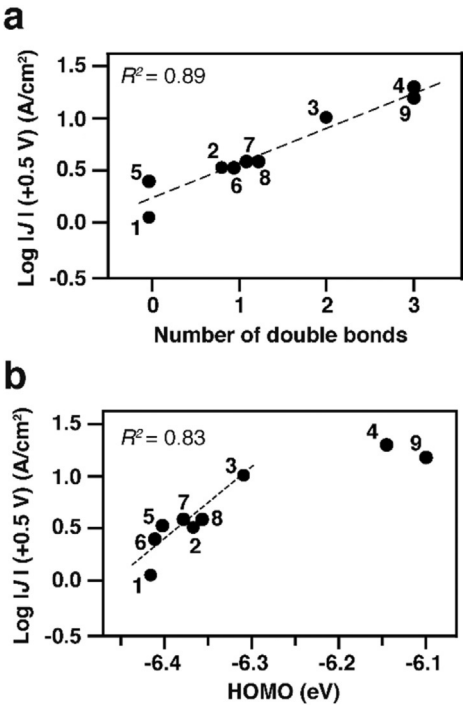


***Figure 3.*** a) Plot of mean values of $\log|J|$ at + 0.5 V grouped by the number of carbon–carbon double bonds for molecules **1**–**9**. Compounds **2**,**6**,**7** and **8** are offset for clarity. b) Plot of mean values of $\log|J|$ at + 0.5 V against the HOMO energy for molecules **1**–**9**. Molecule numbers are listed in the plot. The coefficients of determination ($R^2$) for the dashed lines are shown in the plots.

  

trends support the proposal that the mean decrease in height of the tunneling barrier with unsaturation is primarily responsible for the increase in the tunneling current in going from **1** to **4**.

Tunneling can be surprisingly important when the HOMO is influenced by interacting high-lying occupied molecular orbitals of some chemical groups (lone pairs on amides, ethers).[11] DFT calculations and experimental results suggest that superexchange tunneling may be present in molecule **3**. Further analysis of polyunsaturated hydrocarbons with different relative positions of two or more C=C bonds would be needed before the mechanism of tunneling through these molecules can be firmly established.

These results are not, in our *subjective* opinion, strong enough to establish that the selection of terpenoids as important building blocks for cells by evolution was influenced by their ability to support charge transport. They do suggest that the ability to show CT activity enhanced relative to saturated terpenoids would have required oxidative unsaturation—a process that *might* have occurred in the reducing early earth with oxidizing molecules ($SO_2$, $SO_4$, RSSR, $S_n$, $NO_2$, and $NO_3$) and certain minerals (niter, ferricyanide, and anatase),[21] but would have been more obvious later, as levels of $O_2$ began to rise in a more oxidizing environment. The hydrophobicity of polyisoprenoids, and their chemical stability (relative to polyunsaturated derivatives of fatty acids), could have made them an accessible solution to two problems—formation of stable lipid bilayers and charge transport—at the same time.

## Acknowledgements

We thank Dr. Darrell Collison for his assistance with initial experiments and Prof. Alán Aspuru-Guzik for use of computational resources and helpful discussions. This work was supported by an award from the Simons Foundations (290364), and an award from the National Science Foundation (CHE1808361). We acknowledge the Materials Research and Engineering Center (MRSEC, DMR-1420570) at Harvard University for supporting XPS measurements and providing access to the clean room facilities. Sample characterization was performed in part at the Center for Nanoscale Systems (CNS) at Harvard University, a member of the National Nanotechnology Infrastructure Network (NNIN), which is supported by the National Science Foundation (ECS-0335765)

## Conflict of interest

The authors declare no conflict of interest.

**Keywords:** charge transport · origin of life · quantum tunneling · self-assembled monolayers · terpenes

**How to cite:** *Angew. Chem. Int. Ed.* **2019**, *58*, 8097–8102
*Angew. Chem.* **2019**, *131*, 8181–8186

[1] E. Breitmaier, *Terpenes: Flavors, Fragrances, Pharmaca, Pheromones*, Wiley-VCH, Weinheim, **2006**.
[2] a) G. Ourisson, Y. Nakatani, *Chem. Biol.* **1994**, *1*, 11–23; b) D. W. Deamer, J. P. Dworkin, *Top. Curr. Chem.* **2005**, *259*, 1–27; c) M. Gotoh, A. Miki, H. Nagano, N. Ribeiro, M. Elhabiri, E. Gumienna-Kontecka, A. M. Albrecht-Gary, M. Schmutz, G. Ourisson, Y. Nakatani, *Chem. Biodiversity* **2006**, *3*, 434–455.
[3] a) S. Eberhard, G. Finazzi, F. A. Wollman, *Annu. Rev. Genet.* **2008**, *42*, 463–515; b) J. A. Letts, L. A. Sazanov, *Nat. Struct. Mol. Biol.* **2017**, *24*, 800–808; c) S. H. Light, L. Su, R. Rivera-Lugo, J. A. Cornejo, A. Louie, A. T. Iavarone, C. M. Ajo-Franklin, D. A. Portnoy, *Nature* **2018**, *562*, 140–144.
[4] a) L. M. Barge, Y. Abedian, M. J. Russell, I. J. Doloboff, J. H. Cartwright, R. D. Kidd, I. Kanik, *Angew. Chem. Int. Ed.* **2015**, *54*, 8184–8187; *Angew. Chem.* **2015**, *127*, 8302–8305; b) T. Cardona, P. Sanchez-Baracaldo, A. W. Rutherford, A. W. Larkum, *Geobiology* **2018**, *17*, 127–150; c) M. Yamamoto, R. Nakamura, T. Kasaya, H. Kumagai, K. Suzuki, K. Takai, *Angew. Chem. Int. Ed.* **2017**, *56*, 5725–5728; *Angew. Chem.* **2017**, *129*, 5819–5822.
[5] a) A. Salomon, D. Cahen, S. Lindsay, J. Tomfohr, V. B. Engelkes, C. D. Frisbie, *Adv. Mater.* **2003**, *15*, 1881–1890; b) A. Salomon, T. Boecking, O. Seitz, T. Markus, F. Amy, C. Chan, W. Zhao, D. Cahen, A. Kahn, *Adv. Mater.* **2007**, *19*, 445–450; c) R. L. McCreery, A. J. Bergren, *Adv. Mater.* **2009**, *21*, 4303–4322; d) G. Wang, T.-W. Kim, T. Lee, *J. Mater. Chem.* **2011**, *21*, 18117; e) A. Vilan, D. Aswal, D. Cahen, *Chem. Rev.* **2017**, *117*, 4248–4286; f) D. J. Wold, R. Haag, M. A. Rampi, C. D. Frisbie, *J. Phys. Chem. B* **2002**, *106*, 2813–2816; g) A. Salomon, T. Bocking, J. J. Gooding, D. Cahen, *Nano Lett.* **2006**, *6*, 2873–2876; h) H. J. Yoon, N. D. Shapiro, K. M. Park, M. M. Thuo, S. Soh, G. M. Whitesides, *Angew. Chem. Int. Ed.* **2012**, *51*, 4658–4661; *Angew. Chem.* **2012**, *124*, 4736–4739; i) C. M. Bowers, D. Rappoport, M. Baghbanzadeh, F. C. Simeone, K.-C. Liao, S. N. Semenov, T. Żaba, P. Cyganik, A. Aspuru-Guzik, G. M. Whitesides, *J. Phys. Chem. C* **2016**, *120*, 11331–11337; j) M. M. Thuo, W. F. Reus, F. C. Simeone, C. Kim, M. D. Schulz, H. J. Yoon, G. M. Whitesides, *J. Am. Chem. Soc.* **2012**, *134*, 10876–10884; k) H. J. Yoon, C. M. Bowers, M. Baghbanzadeh, G. M. Whitesides, *J. Am. Chem. Soc.* **2014**, *136*, 16–19; l) C. M. Bowers, K. C. Liao, H. J. Yoon, D. Rappoport, M. Baghbanzadeh, F. C. Simeone, G. M. Whitesides, *Nano Lett.* **2014**, *14*, 3521–3526; m) S. Park, H. J. Yoon, *Nano Lett.* **2018**, *18*, 7715–7718.
[6] J. G. Simmons, *J. Appl. Phys.* **1963**, *34*, 1793–1803.
[7] a) H. M. McConnell, *J. Chem. Phys.* **1961**, *35*, 508–515; b) R. Kosloff, M. A. Ratner, *Isr. J. Chem.* **1990**, *30*, 45–58; c) A. Nitzan, *Annu. Rev. Phys. Chem.* **2001**, *52*, 681–750.
[8] a) C. S. Sangeeth, A. T. Demissie, L. Yuan, T. Wang, C. D. Frisbie, C. A. Nijhuis, *J. Am. Chem. Soc.* **2016**, *138*, 7305–7314; b) C. E. Smith, S. O. Odoh, S. Ghosh, L. Gagliardi, C. J. Cramer, C. D. Frisbie, *J. Am. Chem. Soc.* **2015**, *137*, 15732–15741.
[9] M. Carlotti, M. Degen, Y. Zhang, R. C. Chiechi, *J. Phys. Chem. C* **2016**, *120*, 20437–20445.
[10] S. Y. Sayed, J. A. Fereiro, H. Yan, R. L. McCreery, A. J. Bergren, *Proc. Natl. Acad. Sci. USA* **2012**, *109*, 11498–11503.
[11] a) M. Baghbanzadeh, C. M. Bowers, D. Rappoport, T. Żaba, M. Gonidec, M. H. Al-Sayah, P. Cyganik, A. Aspuru-Guzik, G. M. Whitesides, *Angew. Chem. Int. Ed.* **2015**, *54*, 14743–14747; *Angew. Chem.* **2015**, *127*, 14956–14960; b) M. Baghbanzadeh, C. M. Bowers, D. Rappoport, T. Zaba, L. Yuan, K. Kang, K. C. Liao, M. Gonidec, P. Rothemund, P. Cyganik, A. Aspuru-Guzik, G. M. Whitesides, *J. Am. Chem. Soc.* **2017**, *139*, 7624–7631.
[12] E. A. Weiss, R. C. Chiechi, G. K. Kaufman, J. K. Kriebel, Z. Li, M. Duati, M. A. Rampi, G. M. Whitesides, *J. Am. Chem. Soc.* **2007**, *129*, 4336–4349.

  

[13] a) R. C. Chiechi, E. A. Weiss, M. D. Dickey, G. M. Whitesides, *Angew. Chem. Int. Ed.* **2008**, *47*, 142 – 144; *Angew. Chem.* **2008**, *120*, 148 – 150; b) P. Rothemund, C. Morris Bowers, Z. Suo, G. M. Whitesides, *Chem. Mater.* **2018**, *30*, 129 – 137.
[14] G. F. Joyce, J. W. Szostak, *Cold Spring Harbor Perspect. Biol.* **2018**, *10*, a034801.
[15] E. T. Castellana, P. S. Cremer, *Surf. Sci. Rep.* **2006**, *61*, 429 – 444.
[16] N. Nerngchamnong, L. Yuan, D. C. Qi, J. Li, D. Thompson, C. A. Nijhuis, *Nat. Nanotechnol.* **2013**, *8*, 113 – 118.
[17] L. Yuan, N. Nerngchamnong, L. Cao, H. Hamoudi, E. del Barco, M. Roemer, R. K. Sriramula, D. Thompson, C. A. Nijhuis, *Nat. Commun.* **2015**, *6*, 6324.
[18] F. Furche, R. Ahlrichs, C. Hättig, W. Klopper, M. Sierka, F. Weigend, *Wiley Interdiscip. Rev.: Comput. Mol. Sci.* **2014**, *4*, 91 – 100.
[19] K. C. Liao, H. J. Yoon, C. M. Bowers, F. C. Simeone, G. M. Whitesides, *Angew. Chem. Int. Ed.* **2014**, *53*, 3889 – 3893; *Angew. Chem.* **2014**, *126*, 3970 – 3974.
[20] a) A. D. Becke, *J. Chem. Phys.* **1993**, *98*, 5648 – 5652; b) K. Eichkorn, O. Treutler, H. Öhm, M. Häser, R. Ahlrichs, *Chem. Phys. Lett.* **1995**, *240*, 283 – 290.
[21] S. M. Morrison, S. E. Runyon, R. M. Hazen, *Life* **2018**, 8.

Manuscript received: March 10, 2019
Accepted manuscript online: April 15, 2019
Version of record online: May 8, 2019

  